N87-11210

HIGH-TEMPERATURE CONSTITUTIVE MODELING*

D. N. Robinson and J. R. Ellis
University of Akron

INTRODUCTION

Thermomechanical service conditions for high-temperature structural components, e.g., hot-section aircraft engine and nuclear reactor components, involve temperature levels, thermal transients and mechanical loads severe enough to cause measurable inelastic deformation. Although inelastic strain per cycle is small in many applications (in the order of elastic strain) as cycling occurs in the absence of shakedown inelastic strain can accumulate monotonically (ratchetting) or alternate repeatedly (fatigue). In any case, the seat of failure clearly resides in the occurence of continued inelastic deformation. Structural analysis in support of the design of high-temperature components - leading to the stress, strain and temperature fields upon which life predictions are ultimately based - therefore depends strongly on accurate mathematical representations (constitutive equations) of the nonlinear, hereditary, inelastic behavior of structural alloys at high temperature, particularly in the relatively small strain range. To be generally applicable, constitutive equations must be expressed in multiaxial form and be appropriate for all modes of mechanical and thermal loading to be experienced by the elevated temperature components (e.g., cyclic, non-isothermal, non-radial, etc.).

In contribution to the overall program in constitutive equation development sponsored by the HOST project, the in-house NASA/LeRC effort is concentrating mainly on three fundamental areas of research:

1) Multiaxial experimentation to provide a much needed rational basis for high-temperature multiaxial constitutive relationships.

2) Nonisothermal testing and theoretical development toward a complete thermomechanically path dependent formulation of viscoplasticity - including the influence of thermally induced metallurgical changes.

3) Development of viscoplastic constitutive models accounting for strong initial anisotropy.

Current activities, progress and future directions in these areas of research are indicated in the following sections.

* Work performed under NASA Grant NAG-3-379.

MULTIAXIAL EXPERIMENTATION IN SUPPORT OF CONSTITUTIVE EQUATION DEVELOPMENT

Thoughtful exploratory experimentation must go hand-in-hand with the formulation of constitutive theories and furnish guidance for their development. Without close interaction between experimentalist and theoretician physically unrealistic and ad hoc constitutive models often result that may not be used with confidence even slightly outside the specific conditions addressed by their data base.

A particularly glaring deficiency in terms of elevated temperature testing is that regarding multiaxial behavior. A major reason for this has been the lack of extensometry for accurately measuring multiaxial strain at high-temperature. Only through recent developments in extensometry (e.g., ref.1) has it become possible to do meaningful multiaxial testing at relevant temperatures on relevant materials.

The necessity of conducting fundamental multiaxial tests is best recognized in the context of classical plasticity theory. In that constitutive theory the concept of a yield surface plays a central role. A description of the yield surface, at a fixed inelastic state, together with the concept of normality is precisely that which allows a consistent multiaxial plastic flow law to be expressed. An appropriate description of the yield surface and a demonstration of the validity of the concept of normality can only be realized through multiaxial testing.

At high temperature, alloys of interest are strongly time-dependent (viscoplastic) and the concept of a yield surface, in the classical sense, breaks down. However, concepts have been postulated for time-dependent inelastic behavior that have an analogous geometrical interpretation to that of yield surfaces (e.g., Odqvist (ref.2) and Drucker (ref. 3)). Such a concept was introduced by Rice (ref. 4), Ponter and Leckie (ref. 5) and Ponter (ref. 6) in the form of a flow potential function of the applied stress σ_{ij} and the internal (back) stress α_{ij} *

$$\mathcal{W}(\sigma_{ij},\alpha_{ij}) \tag{1}$$

from which the viscoplastic flow and evolutionary laws are derivable, i.e.

$$\dot{\varepsilon}_{ij} = \frac{\partial \mathcal{W}}{\partial \sigma_{ij}} \tag{2}$$

$$\dot{\alpha}_{ij} = -h(\alpha_{kl})\frac{\partial \mathcal{W}}{\partial \alpha_{ij}} \tag{3}$$

Here, ε_{ij} is the inelastic strain-rate and h is a scalar function of the internal stress. Experimental evidence for the existence of a potential function was found in a preliminary way by Brown (ref.7) and Robinson (ref. 8) and recently and more comprehensively by Oytana, Delobelle and Mermet (ref. 9).

Robinson (refs. 10,11) has adopted a potential function of the general form:**

$$\mathcal{W} = \frac{1}{2\mu}\int f(F)dF + \frac{R}{H}\int g(G)dG \tag{4}$$

---

* As the tests described here are isothermal, the development in this section is similarly limited to isothermal conditions. Also, isotropic hardening effects are taken to be saturated out.

** The complete model utilizes a discontinuous pontential function that allows analytically different governing equations in various "regions of the state space." These aspects of the model will not be discussed here.

in which μ, R and H are material constants (or, under non-isothermal conditions, functions of temperature) and the stress dependence enters through the functions

$$F(\sigma_{ij}, \alpha_{ij}) \text{ and } G(\alpha_{ij}) \tag{5}$$

The flow equation (2) then becomes

$$2\mu\dot{\varepsilon}_{ij} = f(F)\frac{\partial F}{\partial \sigma_{ij}} \tag{6}$$

which can be interpreted geometrically in a superimposed stress and inelastic strain-rate space (fig. 1) as indicating normality of the inelastic strain-rate (vector) to the hypersurfaces

$$F(\sigma_{ij}, \alpha_{ij}) = \text{const.} \tag{7}$$

The internal stress α_{ij}, denoting the inelastic state, is taken fixed. The surface $F = 0$ is considered by Robinson to correspond to a threshold (Bingham-Prager) stress below which the inelastic strain-rate vanishes.

Experimental determination of the function F is analogous to the determination of the yield function (or a yield surface) in classical plasticity. Specification of F at constant inelastic states permits the definition of a consistent multi-axial form of the viscoplastic flow law, and provides information concerning an evolutionary law for the inelastic state variable α_{ij}.

For isotropic alloys it is reasonable to further specialize F and G to be dependent on the principal invariants of the applied and internal stress. In the spirit of v.Mises, Robinson has taken

$$F(J_2) = \frac{J_2}{K^2} - 1 \quad \text{and} \quad G(\hat{J}_2) = \frac{\hat{J}_2}{K^2} \tag{8}$$

as depending on only the second principal invariants

$$J_2 = \frac{1}{2}\Sigma_{ij}\Sigma_{ij} \tag{9}$$

$$\hat{J}_2 = \frac{1}{2}a_{ij}a_{ij} \tag{10}$$

The first of equations (8) plays the role of a (Bingham) yield condition with K denoting the magnitude of the threshold Bingham shear stress.

In equation (9) the effective stress

$$\Sigma_{ij} = S_{ij} - a_{ij} \tag{11}$$

is taken as the difference of the applied deviatoric stress S_{ij} and the internal stress deviator a_{ij}. The choice of stress dependence in equation (8) is consistent with the experimental observations reported in reference 9.

With these choices, equations (2) and (3) give

$$2\mu\dot{\varepsilon}_{ij} = f(F)\Sigma_{ij} \tag{12}$$

and

$$\dot{a}_{ij} = h(G)\dot{\varepsilon}_{ij} - r(G)a_{ij} \tag{13}$$

with

$$\frac{r}{h} = \frac{R}{H}g(G) \tag{14}$$

Evidently, the evolutationary equation (13) is of the physically accepted Bailey-Orowan form.

Squaring both sides of the equation (12) we get

$$4\mu^2 I = f^2 J_2 = \hat{F}(J_2) \tag{15}$$

where

$$I = \frac{1}{2}\dot{\varepsilon}_{ij}\dot{\varepsilon}_{ij} \tag{16}$$

is a measure of the magnitude of the inelastic strain-rate. Equation (15) states (see Fig. 2) that surfaces of constant J_2 in stress space (at a fixed inelastic state) are surfaces of constant inelastic strain-rate I. Further, the strain-rate vectors are normal to these surfaces. Constant inelastic strain-rate surfaces are the counterparts of yield surfaces (surfaces of constant inelastic strain) in time-dependent plasticity.

In general, these surfaces change position and size through changes in the internal stress, threshold stress and time as inelastic deformation and recovery occurs. A complete understanding of the nature and behavior of these surfaces under virgin conditions and conditions subsequent to inelastic deformation (creep, cyclic plasticity, etc.) is prerequisite to formulating a consistent description of multiaxial viscoplastic behavior.

Computer controlled experiments for directly determining the loci of constant inelastic strain rate at fixed inelastic state are included in the test plan for the currently expanding Structures Division laboratory. In the interim period, before that laboratory if fully operational, preliminary tests of this type are being conducted under subcontract to Oak Ridge National Laboratory.

NONISOTHERMAL TESTING AND THERMOMECHANICAL MODELING

Essentially all of the important structural problems related to the design of aircraft engine hot-section components are nonisothermal. Inelasticity does not occur in these components as a result of mechanical loading alone but is generally induced through thermal transient cycles and thermal gradients. Nevertheless, the constitutive equations and life prediction models used in structural analysis and design are almost always based completely on experimental data collected under isothermal conditions. Isothermal tests are commonly conducted over the temperature and then "fit" as functions of temperature across the temperature range to furnish a "nonisothermal" representation. This traditional approach leads to "nonisothermal" models that do not reflect the strong thermomechanical path dependence observed in, for example, the cyclic hardening behavior of some alloys of interest - particularly in the presence of metallurgical changes.

Cyclic hardening of some common structural alloys within their temperature range of interest is believed to be influenced by the phenomenon of dynamic strain aging. Strain aging occurs in solid solutions where solute atoms (e.g., carbon, nitrogen, etc.) are particularly free to diffuse through the parent lattice. It is

energetically preferable for these solute atoms to occupy sites in the neighborhood of mobile dislocations where their presence immobilizes the dislocations or at least makes their movement difficult, thus causing strengthening.

Isothermal cycling at temperatures where such metallurgical changes occur might therefore be expected to show abnormal hardening, i.e., higher hardening rates and greater saturation strengths than at temperatures both lower and higher. Macroscopic evidence of strain aging in three common alloys (i.e., Hastelloy X and types 304 and 316 stainless steel) is shown in figures 3 through 5. In each case the hardening rate and the stress range at "saturation", peak at an intermediate temperature in the range. This hardening peak is interpreted as a manifestation of dynamic strain aging. At lower temperatures the mobility of solute atoms is far less and strain aging cannot occur; at higher temperatures normal recovery precesses, e.g., climb of edge dislocations, take over.

In the aging process described dislocations can, under some circumstances, break away from their solute atmospheres becoming mobile again. Although temporarily freed, dislocations can again be immobilized as solute atoms gradually diffuse back to them. As the thermally activated process of diffusion is involved and solute atoms are migrating to dislocations which themselves are moving under the applied stress, it is expected that the ensuing inelastic deformation (cyclic hardening in particular) has a complex dependence on thermomechanical history.

Phenomenological evidence of thermomechanical path dependence under cyclic conditions is seen in the results of the simple nonisothermal tests reported in figures 3 and 4 (dotted curves). In these tests cycling is initiated at one temperature and after some cycling the temperature is changed and cycling resumed.

Figure 3 shows the results of two nonisothermal tests on Hastelloy X cycled over a strain range at constant strain rate. In one, the specimen is cycled at 800F for five cycles; the temperature is then changed to 1000F and cycling is continued to apparent saturation, at about one hundred cycles. In the second, this history is repeated up to thirty cycles where the specimen is then brought back to 800F and cycling continued. Results of a similar test on type 304 stainless steel are shown in figure 4 (dotted line).

The features of these test results that reflect thermomechanical history dependence are : 1) The change in strength (stress range) with temperature at a fixed number of cycles is always negative, i.e., an increase in temperature always produces a decrease in strength and vice versa, contrary to the implication of the isothermal data; 2) The current strength, in particular the "saturation" strength, depends on the temperature-strain history. Evidently, the information contained in the isothermal data is not sufficient for a complete nonisothermal description of the cyclic deformation in the temperature range of interest. In fact, the data suggests that, with accompanying metallurgical changes, the materials retain a full memeory of their thermomechanical history to cyclic saturation. Similar observations have been made on two-phase alloys (ref.12) presumably arising from microstructural changes associated with precipitation of the γ' phase.

Characterization of isotropic cyclic hardening effects requires that a constitutive model contain a scalar state variable (e.g., K) and a corresponding evolutionary law describing its rate of change with thermomechanical history. A proposed form of evolutionary law appropriate for cyclic stressing (in the absence of thermal recovery) is

$$\dot{K} = \tilde{F}(P,T)\dot{P} + \tilde{G}(P,T)\dot{T} \tag{17}$$

in which

$$P = \int (\dot{\varepsilon}^P_{ij}\, \dot{\varepsilon}^P_{ij})^{1/2} \tag{18}$$

is a measure of the accumulated plastic strain and T is the temperature. The current value of K (or equivalently the stress range) is determined from equation (17) only if the thermomechanical path is known.

Information for characterizing the function $\tilde{F}$ can be obtained from ordinary isothermal tests, however, nonisothermal tests must be conducted to supply information about $\tilde{G}$. Candidate tests for this purpose have been identified and will be conducted as the nonisothermal testing facilities become available in the Structures Division laboratory.

Using preliminary information about the function $\tilde{G}$ an appropriate evolutionary law having the form of equation (17) has been adopted for use with the Robinson viscoplastic model described in references 10 and 11. Predictions made by this nonisothermal model give excellent qualitative agreement with the experimental results of figures 3 through 5.

A VISCOPLASTIC MODEL FOR TRANSVERSE ISOTROPY

The need for increased efficiency in energy systems places greater demands on the high-temperature structural alloys used for system components. As higher operating temperatures are sought, advanced materials are being developed to meet these demands. Good examples of such materials are the directionally solidified polycrystalline alloys finding application in turbine blades of aircraft engines. The directional properties of these metals render them highly anisotropic relative to conventional alloys. This introduces additional complexity in understanding and mathematically representing their mechanical behavior over and above the already enormous complexities associated with elevated temperature.

Here, we discuss a means of extending the isotropic viscoplastic model discussed in the first section and fully described in references 10 and 11 to be applicable to materials with initial anisotropy (ref.13) arising from directionally solidified grain growth.

The direction of grain solidification at each point can be characterized by a field of unit vectors $d_i(x_k)$. The mechanical behavior must then depend not only on the stress and deformation history at the point but also on the local preferential direction. It follows that equation 5 must be replaced by

$$F(\Sigma_{ij}, d_i d_j) \quad \text{and} \quad G(a_{ij}, d_i d_j) \tag{19}$$

In the case of full isotropy F and G were taken as depending on the (second) principal invariants of Σ_{ij} and a_{ij} (eg. (8)). Here instead, we take F and G to depend on invariants that reflect the appropriate anisotropy. The theory of tensorial invariants (ref. 14) requires that for form-invariance under arbitrary rigid-body rotations F and G must be expressible in terms of the principal invariants of their respective tensorial arguments and invariants involving various products of these tensors. Here, we take the functions F and G as depending on subsets of these invariants. We denote I_1, I_2 and I_3 as the invariant arguments of the function F and $\hat{I}_1$, $\hat{I}_2$, $\hat{I}_3$ as those for G.

That is, we take

$$F(I_1, I_2 I_3) = \frac{I_1}{K^2} + \left(\frac{1}{K_d^2} - \frac{1}{K^2}\right)(I_2 - I_3^2) - 1 \tag{20}$$

and

$$G(\hat{I}_1,\hat{I}_2,\hat{I}_3) = \frac{\hat{I}_1}{K^2} + \left(\frac{1}{K_d^2} - \frac{1}{k^2}\right)\left(\hat{I}_2 - \hat{I}_3^2\right) \tag{21}$$

where

$$\begin{aligned} I_1 &= \tfrac{1}{2}\,\Sigma_{ij}\Sigma_{ji} & \hat{I}_1 &= \tfrac{1}{2}\,a_{ij}a_{ji} \\ I_2 &= d_i d_j \Sigma_{jk}\Sigma_{ki} & \hat{I}_2 &= d_i d_j a_{jk} a_{ki} \\ I_3 &= \tfrac{1}{2} d_i d_j \Sigma_{ji} & \hat{I}_3 &= \tfrac{1}{2}\, d_i d_j a_{ji} \end{aligned} \tag{22}$$

As before, the flow and evolutionary equations are obtained by taking the appropriate derivatives as indicated in equations (2) and (3). This results in

$$2\mu\dot{\varepsilon}_{ij} = f(F)\left[\Sigma_{ij} + \left(\frac{K^2}{K_d^2} - 1\right)\left(d_j d_k \Sigma_{ki} + d_k d_i \Sigma_{jk} - \tfrac{1}{2}\, d_p d_k \Sigma_{kp}(\delta_{ij} + d_i d_j)\right)\right] \tag{23}$$

for the flow law, and

$$\dot{a}_{ij} = h(G)\dot{\varepsilon}_{ij} - r(G)\left[a_{ij} + \left(\frac{K^2}{K_d^2} - 1\right)\left(d_j d_k a_{ki} + d_k d_i a_{jk} - \tfrac{1}{2}\, d_p d_k a_{kp}(\delta_{ij} + d_i d_j)\right)\right] \tag{24}$$

for the evolutionary law.

As earlier, K denotes the threshold (Bingham) shear stress transverse to the preferential material direction. K_d denotes the same for shear along the material direction. For $K = K_d$, indicating no difference in shear strength across and along the direction d_i, equations (23) and (24) reduce to their respective isotropic counterparts eqs. (12) and (13).

Equations 20 through 24 have been applied in several structural problems involving creep and cyclic plasticity. The predictions give good qualitative agreement with existing experimental results on the directionally solidified (DS) alloy MAR-M-247 as reported in reference 14. Quantitative comparisons are delayed until characterization tests on a DS alloy furnish specific values of the material parameters in the viscoplastic model.

Additional studies are continuing concerning the adoption of other sets of invariants (integrity bases) reflecting higher degrees of anisotropy, e.g., orthotropy and cubic symmetry.

REFERENCES

1. Ellis, J.R., "A Muliaxial Extensometer for Measuring Axial, Torsional and Diametral Strains at Elevated Temperature", ORNL/TM 8760, (1983).

2. Odqvist, F.K.G., "Recent Advances in Theories of Creep of Engineering Materials", Applied Mechanics Reviews, 7, pp. 517-519, (1954).

3. Drucker, D.C., "On Time-Independent Plasticity and Metals Under Combined Stress at Elevated Temperature", Brown University Report NONR 562(20)/46, (1965).

4. Rice, J.R., "On the Structure of Stress-Strain Relations for Time-Dependent Plastic Deformations in Metals", J. Appl. Mech., Trans, ASME 37, Series E. No. 3, 728-37, (1970).

5. Ponter, A.R.S. and Leckie, F.A., "Constitutive Relationships for the Time-Dependent Deformation of Metals", J. Eng. Mater, Technol., Trans. ASME 98, 47-51 (1976).

6. Ponter, A.R.S., "Convexity and Associated Continuum Properties of a Class of Constitutive Relationships", J. de Mecanique 15 (4), 527-42 (1976).

7. Brown, G.M., "Inelastic Deformation of an Aluminum Alloy Under Combined Stress at Elevated Temperature", J. Mech. Phys. Solids 18, 383-396 (1970).

8. Robinson, D.N., "On the Concept of a Flow Potential and the Stress-Strain Relations of Reactor Systems Metals". ORNL/TM 5571, (1976.

9. Oytana, C., Delobelle, P., and Mermet, A., "Constitutive Equations Study in Biaxial Stress Experiments", J. of Eng'r. Materials and Tech., Vol. 104, pp. 1-11, (1982.

10. Robinson, D.N., "A Unified Creep-Plasticity Model for Structural Metals at High Temperature". ORNL/TM 5969, (1978.

11. Robinson, D.N. and Swindeman, R.W., "Unified Creep-Plasticity Constitutive Equations for 2-1/4 CR-1 Mo Steel at Elevated Temperature." ORNL/TM 8444, (1982).

12. Cailletaud, G. and Chaboche, J.-L, "Macroscipic Description of the Microstructural Changes Induced by Varying Temperature: Example of IN 100 Cyclic Behavior", ICM, 3, Vol. 2 (1979).

13. Robinson, D.N., "Constitutive Relationships for Anisotropic High-Temperature Alloys", NASA Technical Memorandum 83437, presented at the International Post-Conference Seminar on Inelastic Analysis and Life Prediction, Chicago, (1983).

14. Sink, S.W., Hoppin, G.S. and Fuji, M., "Low Cost Directionally-Solidified Turbine Blades", Vol. 1, NASA CR-159464 (1979).

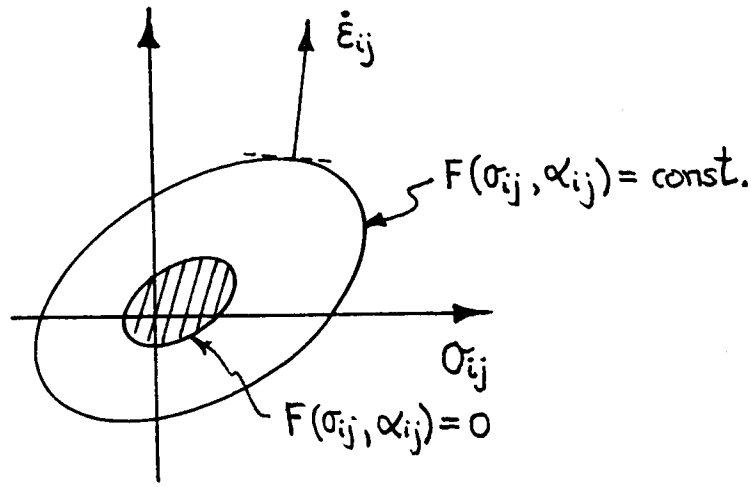

Figure 1 Flow potential surfaces in stress space showing normality of inelastic strain rate vectors.

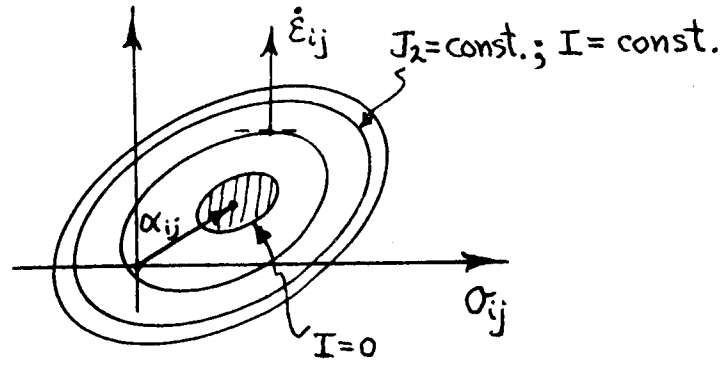

Figure 2 For an isotropic J_2 material ,surfaces of constant inelastic strain rate are surfaces of J_2 = constant.

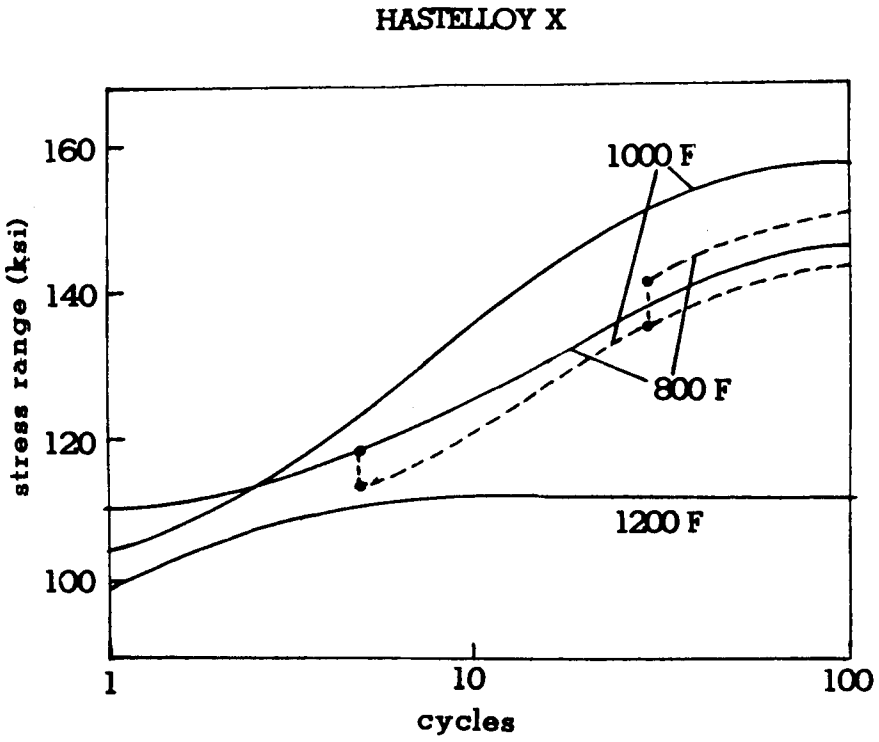

Figure 3 Isothermal(solid)and nonisothermal(dotted) cyclic hardening curves for Hastelloy X.

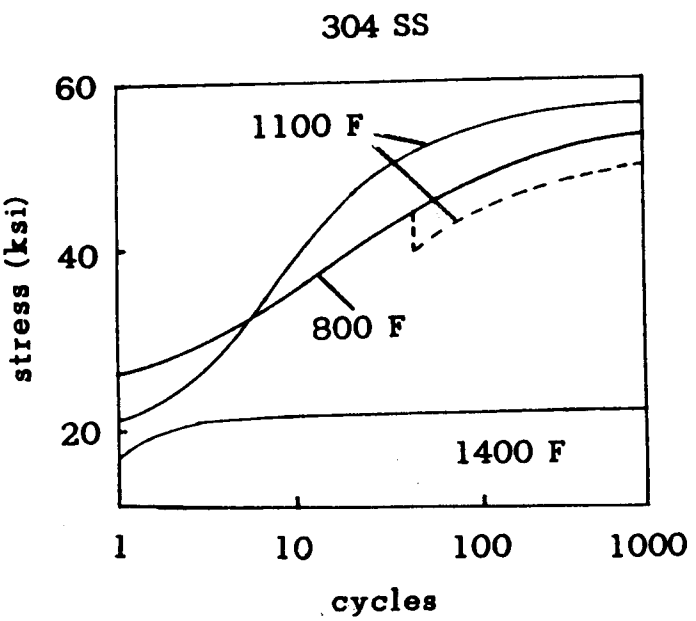

Figure 4 Isothermal(solid)and nonisothermal(dotted) cyclic hardening curves for type 304 Stainless Steel.

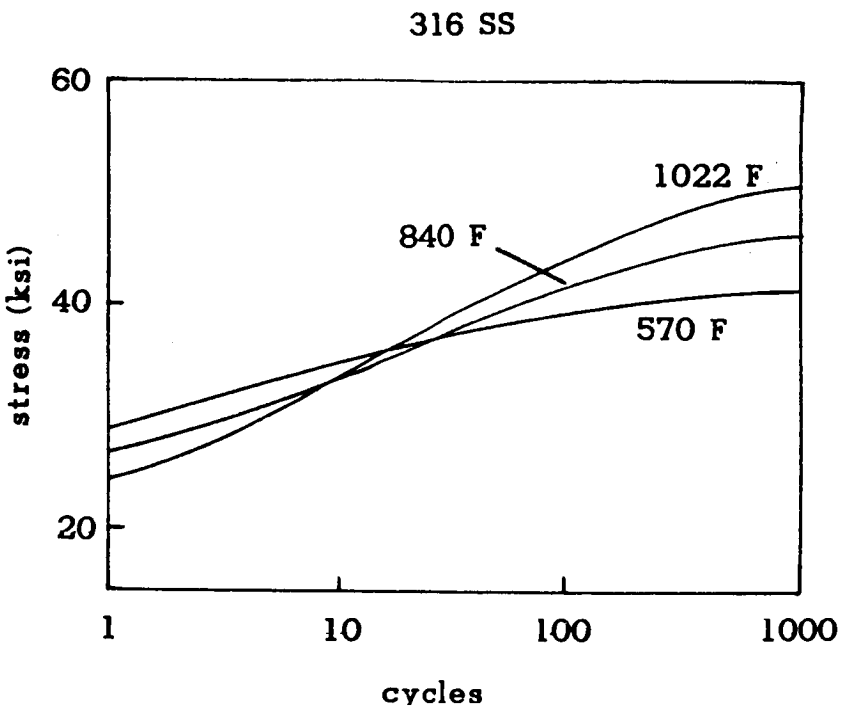

Figure 5 Isothermal cyclic hardening curves for type 316 Stainless Steel.